17th Australasian Fluid Mechanics Conference
Auckland, New Zealand
5-9 December 2010

LES of a Passive Control for Vortex Shedding from Bluff Bodies: Comparisons with Experiments and Near Wake Topology

Andrew A. Antiohos, S. Eren Semercigil and Özden F. Turan

School of Engineering and Science
Victoria University, Melbourne, Victoria 8001, AUSTRALIA

Abstract

A passive control is numerically investigated in this paper to effectively suppress the vortex shedding from bluff bodies. To implement the control, three sinusoidal leading edge configurations are considered and compared to a straight square cylinder case. Large Eddy Simulation (LES) is used to model the wall effects, as well as the near wake.

Numerical velocity fluctuations in the near wake compare well with experimental data. The LES observations provide an accurate prediction of wake instability and near wake topology, otherwise not provided experimentally. This advantage can be used for further investigation of a thorough understanding and enhancement of control.

Numerical case studies are presented using the software package *FLUENT* and the observations are presented in the form of design charts, as well as velocity spectra and near wake flow details.

Introduction

The study of vortex shedding from bluff bodies is important, particularly for industrial applications where efficiency and performance are main design criteria. In order to enhance the aerodynamic properties of a given structure in cross-flow an understanding of the flow dynamics must be established, allowing the design of a control for vortex shedding. Some structures that require effective improvement of their aerodynamic performance in cross-flow can include airfoils, cylindrical support structures, as well as turbo-machinery components, such as jet engine and wind turbine blades.

In order to control vortex shedding, application of passive devices to the structures is common, as this provides effective solutions without the need for external energy resources. An example of the use of passive devices include some recent work by Bearman and Brankovic [1], in which strakes and bumps have been used on circular cylinders to control vortex shedding and effectively reduce vortex induced vibration.

An effective application to control vortex shedding and improve aerodynamic performance of a structure is the introduction of a wavy leading edge on a bluff body implemented by Bearman and Owen [2]. They concluded up to 30% reduction in drag and complete suppression of vortex shedding as compared to a straight leading edge. Darekar and Sherwin [3] also reported drag reductions with a wavy leading edge applied to a square cylinder and determined as a result, that the near wake appeared uniform in nature.

The objective of this paper is to present numerical observations of the flow field around a square cylinder with a wavy leading edge. Comparisons are made particularly with the experimental work of Dobre *et al.* [5], which investigates the effectiveness of different configurations of a sinusoidal periodic perturbation method (SPPM) on square cylinders. Validity of the numerical observations is determined, in order to commence additional investigations into this type of vortex shedding control.

Model Description

The full computational domain for the numerical simulations is presented in Figure 1(a). The domain is similar to that used by Saha *et al.* [7], as it ensures sufficient space for the downstream wake development, as well as minimising blockage effects due to boundaries in the y-direction. It extends from the center of the cylinder a distance of 7*D* both upstream and along the y–direction and a distance of 15*D* downstream.

Four models of a square cylinder were considered for numerical analysis, which are similar to the experimental models of Dobre *et al.* [5]. The models are a plain square cylinder for reference comparisons and three additional models, each with a different configuration of the passive sinusoidal periodic perturbation method (SPPM) applied at the leading edge (LE). Similar to [5], the three SPPM models are referred to as *W*1, *W*2 and *W*3 containing peak–to–peak sinusoidal amplitudes, ω, of 2, 8 and 15 mm, respectively. *W*0 refers to the reference square cylinder. *W*0 and *W*3 are presented in Figure 1(b). The wavelength, λ, of the

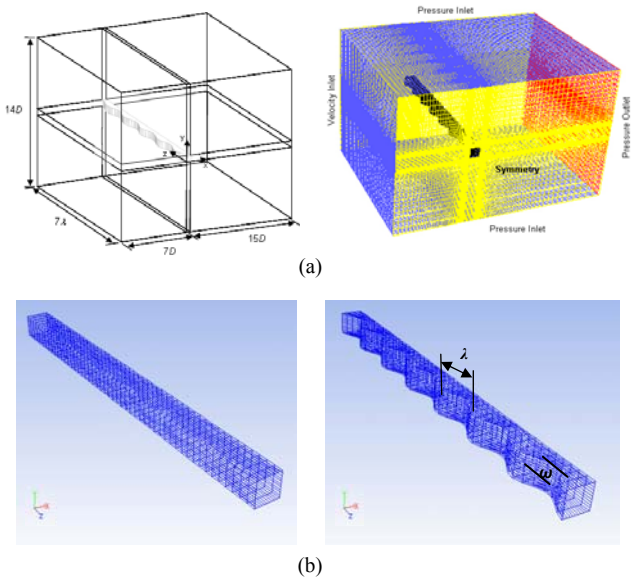

Figure 1: Numerical domain for the square cylinder; (a) Domain schematic and boundary conditions with computational mesh; (b) Reference square cylinder and square cylinder with SPPM applied.

applied SPPM was fixed at a value of 76.8 mm for each configuration. Therefore, *W*1, *W*2 and *W*3 had steepness ratios, ω/λ, of 0.026, 0.105 and 0.197, respectively.

FLUENT has been used to perform the numerical simulations using Large eddy Simulation (LES). The velocity inlet boundary condition was set at a fixed value of U_o = 11 ms^{-1}, corresponding to a Reynolds number, $Re = U_oD/v$, of 2.35×10^4, where D is the cylinder height and v is the kinematic viscosity. This inlet condition is equivalent to the experimental inlet condition of [5]. Pressure inlet boundary conditions were applied to the top and bottom boundaries and a pressure outlet boundary condition was applied to the downstream boundary, as shown in Figure 1(a). The model is three-dimensional and assumed that the square cylinder is infinite along the span. Therefore, in order to reduce the computational requirements, the span length was 7λ, and the side planes were given as symmetry boundaries.

LES requires a sufficiently small time step for resolving the momentum and energy equations and to accurately capture the vortex shedding. This can delay the solution from reaching convergence. Therefore, before starting the LES simulations, initial convergence of the numerical solution was obtained through the Standard–$k\varepsilon$ (SKE) turbulence model. The SKE solution converged at approximately 2000 iterations. This provided the LES model with sufficient reference values to reach faster convergence. Initially, the time step size, dt, for the LES was 1×10^{-5} sec. Once achieving convergence at approximately 0.1 sec of simulation run time, the time step was changed to 1×10^{-4} sec and the LES was completed within a total simulation time of 2 sec. This process improved the performance of the simulations, while considering the fine computational mesh required for LES and ensuring accuracy of the solution. Convergence was indicated from the number of iterations required per time step and through monitoring the residuals.

The mesh used is a structured hexahedron mesh of 345000 cells, the maximum allowable mesh given the hardware and software. A size function was used starting from the cylinder wall, in order to ensure a fine enough mesh to sufficiently resolve the boundary layer, while minimising the effect on computational time. The resulting mesh is shown in Figure 1(a). The value of wall y^+ defined as $y^+ = u_\tau y/v$, where u_τ is the friction velocity at the wall and y is the distance between the wall and adjacent cell centroid, is between 11 and 16 for the models. As this value of y^+ is within the buffer layer an enhanced wall function was applied, given as, $u^+ = e^{\Gamma}u^+_{lam} + e^{1/\Gamma}u^+_{turb}$, where $\Gamma = -0.01(y^+)^4 / (1 + 5y^+)$, in order to blend the law-of-the-wall and log-law regions.

Numerical Observations

Near Wake Analysis

The effectiveness of the SPPM on the near wake of the square cylinder was analysed experimentally by Dobre *et al.* [5] at a location equal to (x/D, y/D) = (2, 2). Measurements were obtained at the midpoint along the span for *W*0; whereas, measurements were obtained at the midpoint peak and valley locations of the wavy LE for *W*1, *W*2 and *W*3. A peak and valley correspond to the most downstream and most upstream LE amplitudes, respectively. Power spectral densities (PSD) of the v-velocity fluctuations are presented in Figure 2. The present numerical observations compare well with the experimental results of [5].

Both experimental and numerical PSD indicate a fundamental harmonic at approximately 47 Hz, corresponding to the vortex shedding frequency, f_{vo}. Therefore, the Strouhal number for the square cylinder at this Reynolds number is $St = f_{vo}D/U_o$ of 0.14. This is in good agreement with typical values of St for a square cross-section. The presence of a first harmonic in Figures 2(a) and 2(b) indicate some radial asymmetry of the vortices in the near wake [5]. This first harmonic is present in the comparisons for Figures 2(a) to 2(c), whereas the fundamental and first harmonics are suppressed for *W*3 in Figure 2(d). The v-velocity spectra for both experimental and numerical results in Figure 2 follow the negative 5/3 slope corresponding to Kolmogorov's law. This region of local isotropy is indicated by the straight line above the spectra. Both comparisons show larger reductions in velocity fluctuations at a valley location. The numerical observations show the effectiveness of the SPPM as steepness ratio increases from *W*0 to *W*3, as indicated by the decreasing fundamental harmonic peak in Figures 2(a) to 2(d).

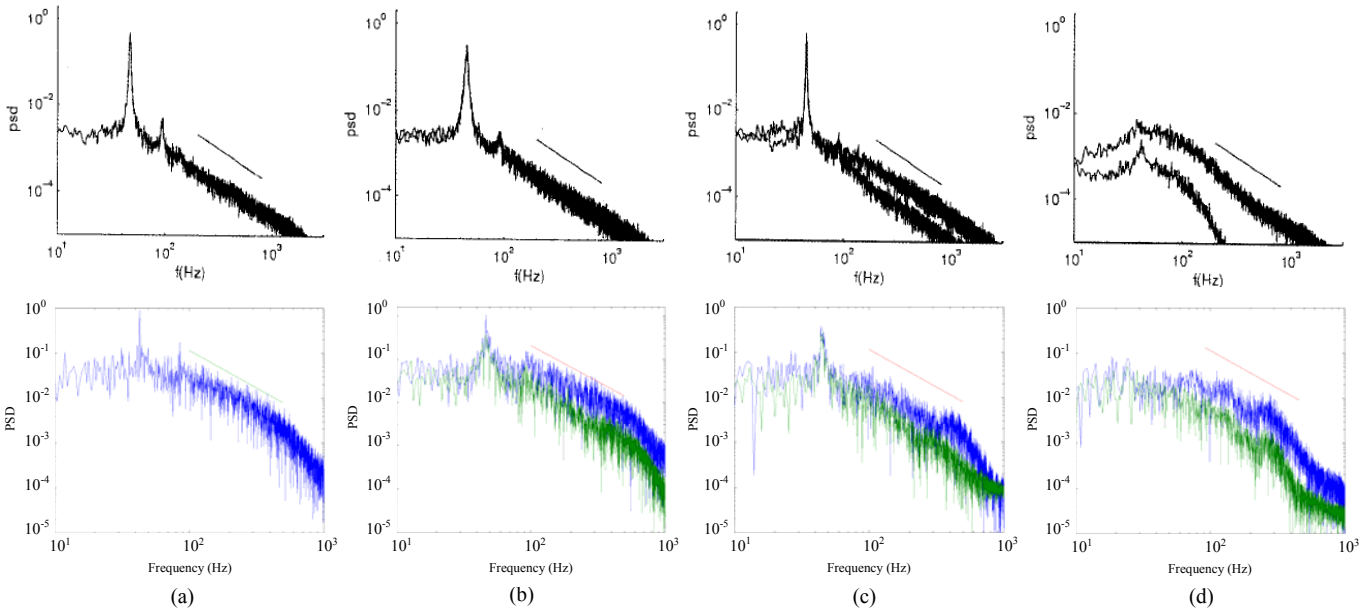

Figure 2: PSD of the v component velocity spectra at peak (——) and valley (——) locations measured at (x/D, y/D) = (2.5, 2.5). Comparisons between experimental (---- Dobre, Hangan and Vickery [4]) and numerical observations for (a) *W*0; (b) *W*1; (c) *W*2 and (d) *W*3.

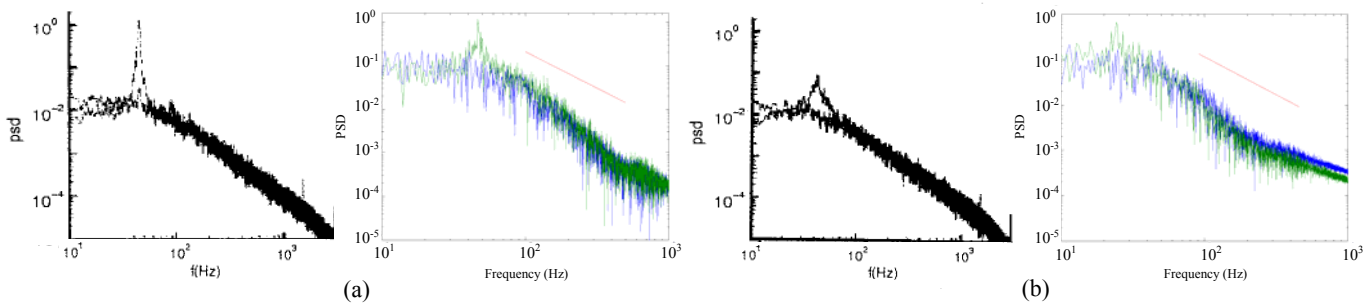

Figure 3: PSD of the u-component (----) and υ-component (----) velocity spectra at the centerline peak location of (x/D, y/D) = (9, 0). Comparisons between experimental (---- Dobre, Hangan and Vickery [5]) and numerical observations for (a) W1 and (b) W3.

Darekar and Sherwin [3] conducted a parametric space study, which classifies each SPPM configuration into three flow regimes. Regime I, corresponding to $W1$ shows slight three-dimensionality in the near wake formation with similar force patterns to $W0$. Regime II, corresponding to $W2$ contains a large spanwise curvature in the top and bottom shear layers, following the SPPM pattern with a decrease in the drag and lift forces. In regime III, the near wake is completely steady with no presence of Kármán vortices and significantly reduced mean drag and lift forces.

The PSD results in Figure 2 indicate the three flow regimes of [3]. In Figure 2(d) complete suppression of vortex shedding is shown with $W3$, indicated by the absence of the spectral peaks. For $W2$, the decrease in magnitude of the fundamental harmonic and suppression of the first harmonic for the numerical observations indicate the presence of regime II. Therefore, the effect of the SPPM at ω/λ of 0.105 appears to benefit the development of the near wake of $W0$. Bearman and Owen [2] obtained complete suppression of vortex shedding for ω/λ in excess of 0.09, in good agreement with [5] and the numerical observations at ω/λ of 0.197 within regime III. This indicates that large wave steepness is required for vortex shedding control.

Intermediate Wake Analysis

In the intermediate wake, the effectiveness of the SPPM is still present. Dobre *et al.* [5] analysed the intermediate wake at a location equal to (x/D, y/D) = (9, 0) to determine the rate of vorticity decay produced by the application. They determined a spanwise homogeneity between the spanwise peak and valley locations; and therefore, only considered the midpoint peak for analysis.

The experimental and numerical comparisons for PSD of the u and v-velocity fluctuations are presented in Figure 3(a) for $W0$ and Figure 3(b) for $W3$ at the midpoint peak location. Larger, green peaks correspond to the v-velocity fluctuations. It can be seen that $W3$ maintains the reduction of vortex shedding. However, a slightly higher magnitude in PSD spectra exists, as compared to the near wake observations of Figure 2(d). This can be due to the interaction between the top and bottom shear layers at the wake centerline at (x/D, y/D) = (9, 0). An indication of significant three-dimensionality within the wake of $W3$ appears from the broad spectral peak in Figure 3(b). The reduction in magnitude is an indication of the lower energy of the vortices, as compared to $W0$ [5]. The numerical PSD of Figure 3(b) shows a shift in the fundamental harmonic peak, which can be due to the suppression of vortices. The reason for the lower energy of vortices and flow three-dimensionality with $W3$ configuration is due to interactions between primary and secondary vortex structures [4, 5]. These structures are the spanwise Kármán vortices and streamwise interconnecting ribs, respectively.

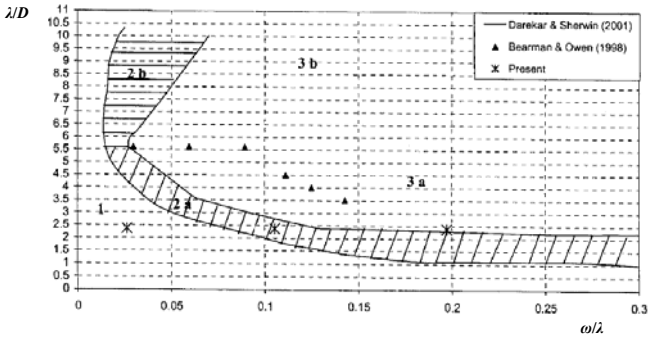

Figure 4: Flow regimes for a square cylinder with a sinusoidal leading edge (Dobre, Hangan & Vickery [5]).

Flow Regimes and Characteristics

In Figure 4, the three flow regimes of [3] are presented parametrically with comparisons between [2, 3 and 5]. The vertical and horizontal axes represent the normalised wavelength, λ/D, and wave steepness, ω/λ, respectively. As in [5], the fixed wavelength of 76.8 mm and variable ω/λ utilised in the numerical analysis ensures all three flow regimes are considered. This approach also selects the wave steepness of $W3$ to become the nominal wave steepness for obtaining flow regime III and achieving vortex suppression.

Reductions in drag coefficient, C_d, of up to 30 percent with a steepness ratio ω/λ in excess of 0.09 are suggested in [2, 3 and 5]. The present numerical results are presented in Table 1 for drag coefficient, C_d. It can be seen that the average values of C_d decrease with increasing wave steepness. However, only 10.3 percent decrease in C_d occurs between $W1$ and $W2$, which indicates only slight effectiveness with mild wave steepness. Increasing the wave steepness further to ω/λ of 0.197, corresponding to $W3$ obtains a reduction in C_d of 31.3 percent from the reference square cylinder. This is a significant improvement in drag reduction and in good agreement with the published results.

Configuration	Average	C_d Reduction [%]
$W0$	0.04	N/A
$W1$	0.039	1.5
$W2$	0.035	13
$W3$	0.028	31.3

Table 1: Drag coefficient, C_d, data for the numerical observations.

Near Wake Topology

In order to verify the effectiveness of the SPPM and determine an understanding of the flow dynamics, a near wake topology analysis was conducted. As the most effective application of the SPPM occurred for ω/λ of 0.197, which corresponds to *W*3, the topology study was obtained with comparisons between the reference case, *W*0, and *W*3. Contours of vorticity are given along the trailing edge (TE) plane in Figure 5(a), and spanwise planes, corresponding to peak and valley locations in Figure 5(b). The images of Figure 5 are obtained at a simulation run time of approximately 2.15 sec, at an instance corresponding to a converged solution. The colour scale represents the magnitude of vorticity with the largest magnitude located along the upper and lower corners of the LE.

In Figure 5(a), the vorticity contours along the TE plane contain a transverse wave occurring for *W*0; whereas, a standing wave is obtained along the span of *W*3 configuration. This suggests that the interaction between the primary vortex structures themselves and primary to secondary structures are minimised with *W*3.

Complete suppression of vortex shedding is achieved with the large sinusoidal amplitude and steepness ratio of *W*3. This is confirmed in Figure 5(b), as clear vortex shedding occurs for *W*0, whereas a consistent streamwise flow pattern exists for *W*3. The vortex structure for *W*0 appears to be uniform along the span of the cylinder. However, slight variation in the shedding instance for each plane along the span exists. The propagating wave along the span can be due to this variation in shedding instance. As the cross-section of *W*0 is uniform, the position and pattern of developing spanwise von Kármán vortices remain constant.

There is no indication of vortex shedding within the wake of *W*3 and the contours along the spanwise planes confirm the occurrence of the standing wave at each plane. As the constant stream of flow over the cylinder has no vortex shedding and hence, no variation in shedding instance, the transverse wave along the spanwise direction is prevented.

El-Gammal, Hangan & King [6] studied the effectiveness of the SPPM on a dynamic bridge section model using surface pressure measurements. Their results showed an increase in the steadiness

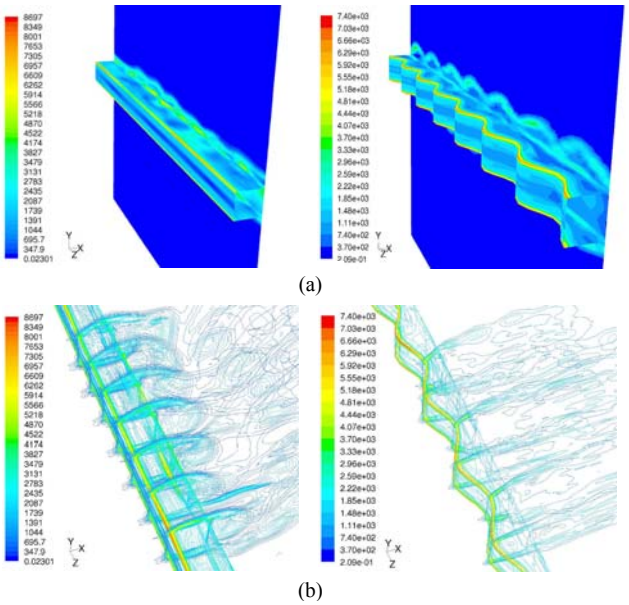

(a)

(b)

Figure 5: Contours of vorticity magnitude for (a) TE plane of (left) *W*0 and (right) *W*3; (b) Spanwise peak and valley planes of (left) *W*0 and (right) *W*3.

of the attached flow along the bridge surface. They also concluded that suppression of vortex shedding was achieved for ω/λ of 0.19, as discussed in the near wake analysis for *W*3. In Figure 5(b), flow attachment is shown at each valley plane and an absence of identifiable vortices throughout the span of *W*3, in agreement with [6].

Three-dimensional wake characteristics in the near to intermediate regions are associated with vortex wake instabilities, which define the interactions between primary and secondary structures. For *W*3, the sharp flow separation at the LE at each peak location and the flow attachment at every valley location suggests that the formation of the interconnecting ribs is prevented; therefore, suppressing the evolution of spanwise Kármán vortices.

Conclusion

Comparisons have been made between experimental and numerical observations of velocity spectra in the near and intermediate wakes of a square cylinder with and without a wavy leading edge. Complete suppression of vortex shedding and velocity fluctuations have been obtained for a steepness ratio ω/λ of 0.197, in good agreement with the corresponding flow regime.

Analysis of the near wake topology through visualisation of the vorticity contours confirms both the effectiveness of the SPPM and results for velocity spectra. Large wave steepness creates an almost uniform flow field and an almost steady span-wise distribution over the cylinder with attached flow along valley planes. This establishes an understanding of the connections between the primary and secondary vorticity structures.

The similarities between experimental and numerical analysis indicate the suitability of the numerical method. Accurate flow details and predictions can be obtained for studying the dynamics of this particular control technique for vortex shedding.

References

[1] Bearman, P. & Brankovic, M., Experimental Studies of Passive Control of Vortex-Induced Vibration, *European Journal of Mechanics B/Fluids*, **23**, 2004, 9-15.

[2] Bearman, P.W. & Owen, J.C., Reduction of Bluff-Body Drag and Suppression of Vortex Shedding by the Introduction of Wavy Separation Lines, *Journal of Fluids and Structures*, **12**, 1998, 123-130.

[3] Darekar, R.M. & Sherwin, S.J., Flow Past a Bluff Body with a Wavy Stagnation Face, *Journal of Fluids and Structures,* **15**, 2001, 587-596.

[4] Dobre, A. & Hangan, H., Investigation of the Three-Dimensional Intermediate Wake Topology for a Square Cylinder, *Experiments in Fluids*, **37**, 2004, 518-530.

[5] Dobre, A., Hangan, H. & Vickery, B., Wake Control Based on Spanwise Sinusoidal Perturbations, *AIAA*, **44**, 3, 2006, 485-492.

[6] El-Gammal, M., Hangan, H. & King, P., Control of Vortex Shedding-Induced Effects in a Sectional Bridge Model by Spanwise Perturbation Method, *Journal of Wind Engineering and Industrial Aerodynamics*, **95**, 2007, 663-678.

[7] Saha, A. K., Biswas, G. & Muralidhar, K., Three-Dimensional Study of Flow Past a Square Cylinder at Low Reynolds Numbers, *International Journal of Heat and Fluid Flow*, **24**, 2003, 54-66.